Journal of Sound and Vibration (1997) **201**(5), 577–593

OPTIMIZATION OF AN ACTIVE NOISE CONTROL SYSTEM USING SPHERICAL HARMONICS EXPANSION OF THE PRIMARY FIELD

T. Martin and A. Roure

Laboratoire de Mécanique et d'Acoustique, 31 *chemin Joseph Aiguier*, 13402 *Marseille cedex* 20, *France*

(*Received* 1 *October* 1995, *and in final form* 14 *October* 1996)

The design of an active noise control system involves several steps. One of the most important is to find the best locations of the control sources and error sensors according to the primary source distribution and its spectrum. Thus the first step in this optimization problem is to obtain an analytical expression for the primary sound field. In this work this was done by using a spherical harmonics expansion, determined on the basis of measurements of the primary field. It is shown how, by using such an expansion, a method can be developed for optimizing the transducer locations for the case of free field radiation of a period general primary source. Finally it is shown how this measurement database can be used to choose a good compromise between the number and the locations of the error sensors.

© 1997 Academic Press Limited

1. INTRODUCTION

The inherent constraints in designing an active noise control system are numerous. In practice, one has to decrease significantly the noise emitted by any primary source by using a few suitably placed actuators and sensors. Furthermore, the number and strengths of the control sources must not be prohibitive. Hence one needs to compromise between what is efficient and what is realistic. In addition, the spectral complexity of some noise sources adds further problems. Moreover, it is very difficult to optimize transducer locations in a general case. The focus in this paper is on the case of a harmonic stationary primary source radiating in a free field. An electric transformer is a good example of such a source but other industrial acoustic sources (compressor, fan noise, etc.) with well-defined spectral components can be dealt with by the method proposed. Many active control experiments have been done on this source type. The studies of Conover and Ringlee [1] on a 150 MVA transformer gave good results, but in restricted directions. With three loudspeakers and three microphones, Kido and Onoda [2] achieved a 25 dB reduction of the 100 Hz component in certain directions, but an increase in sound level elsewhere. Ross conducted experiments *in situ* with only one loudspeaker [3]. By displacing the loudspeaker and estimating the efficiency at many points of a room 20 m away, he found that the lowest frequency (100 Hz) was uniformly and efficiently controlled (10–20 dB), while the highest harmonics were less and only locally controlled. He concluded that this very simple system gives significant noise reduction, but that the number of loudspeakers should be increased. Other work done with different control sources [4, 5] gave either good results only in

0022–460X/97/150577 + 17 $25.00/0/sv960782 © 1997 Academic Press Limited

certain directions or an omnidirectional reduction, but at the price of too many control sources. The theoretical approaches of active noise control in free field are multifarious. Nelson and Elliott [6, 7] used a global approach by minimizing the total power output of a set of primary and secondary point sources. Kempton [8] developed the primary field of a point source in a Taylor series, which led him to use a set of multi-polar sources as secondary sources located at a distance d from the primary source. The approach used here resembles that of Kempton. This method, first developed by Filippi and Piraux [9–11], consists of noise source modelling by a spherical harmonics expansion. Some advantages in using the spherical harmonics expansion over Kempton's approach are that there are fewer less series terms (cf., [12]), and that decomposition of any primary field can be done, whereas Kempton's technique is for a point source.

In what follows, this method is used to determine the number and the positions of the control sources at different points. The next step is to use the previously defined control source distribution to minimize the sum of the squared pressures at a number of error sensors and to decrease progressively the number of sensors.

2. ACOUSTIC FIELD IDENTIFICATION BY MEANS OF SPHERICAL HARMONICS FUNCTIONS

Many studies [9–11] have shown that the acoustic field radiated by a source can be accurately approximated by using a representation in the form of a finite sum of spherical harmonics functions. The aim of this study was to apply this method to active noise control. By limiting the truncation order of the mathematical models used and by identifying each term of the series as due to a particular multipolar-type source [7, 12, 13], one may design an easy-to-implement system because of the limited number of elements.

2.1. MODELLING AND ASSOCIATED MINIMIZATION PROBLEMS

Consider a sound source occupying a volume V, radiating in free field. With a harmonic time dependence ($e^{-i\omega t}$), and outside V, the sound pressure at point M satisfies

$$\left\{\begin{array}{l}(\Delta + k^2)p(M) = 0\\ \text{Sommerfeld conditions}\end{array}\right\}.$$

Let (R, θ, ϕ) be the spherical co-ordinates of point M in spherical co-ordinate system of origin O. Let Σ be the smallest sphere centered at O containing V. Outside Σ, $p(M)$ can be expanded into a spherical harmonics series as

$$p(M) = \sum_{n=0}^{\infty} \mathrm{h}_n(kR) \sum_{m=0}^{n} A_{nm} \mathrm{P}_n^m(\cos\theta) \cos m\phi$$

$$+ \sum_{n=1}^{\infty} \mathrm{h}_n(kR) \sum_{m=0}^{n} B_{nm} \mathrm{P}_n^m(\cos\theta) \sin m\phi, \qquad (1)$$

where $\mathrm{h}_n(kR)$ is the spherical Hankel function of the first kind corresponding to outgoing waves, and $\mathrm{P}_n^m(z)$ is the Legendre function of degree n and order m.

More generally, one can consider a set of points O_j and spheres Σ_j centered at these points and containing V. With (R_j, θ_j, ϕ_j) as the co-ordinates of point M in the co-ordinate

system centered at O_j, one sees [9, 11] that outside any closed surface containing all the spheres Σ_j, $p(M)$ can be expanded as

$$p(M) = \sum_{j=1}^{n_c} \left[\sum_{n=0}^{\infty} \mathrm{h}_n(kR_j) \sum_{m=0}^{n} A_{nm}^j \mathrm{P}_n^m(\cos\theta_j) \cos m\phi_j + \sum_{n=1}^{\infty} \mathrm{h}_n(kR_j) \sum_{m=1}^{n} B_{nm}^j \mathrm{P}_n^m(\cos\theta_j) \sin m\phi_j \right], \tag{2}$$

where n_c is the number of acoustical centers O_j.

Suppose that the pressure $\tilde{P}(M_i)$ is known at N points surrounding the source. By establishing a mathematical representation of the sound pressure $p(M_i)$ at these points, one can determine the representation parameters by a least squares method. With each model one can associate the following minimization problem:

$$\left.\begin{array}{l} \text{Find the parameters } A_{nm}^j \text{ and } B_{nm}^j \text{ such that the functional} \\ J = \sum_{i=1}^{N} |P(M_i) - \tilde{P}(M_i)|^2 \text{ is minimum} \end{array}\right\}. \tag{3}$$

For a single center O, $P(M_i)$ is the series (1) truncated at the selected order, or the series (2) for several centers O_j ($j = 1, \ldots, n_c$). In the latter case, one has to define a set of integers N_j representing the truncation order of each series associated with the center O_j. $(R_{ij}, \theta_{ij}, \phi_{ij})$ are the co-ordinates of each point M_i in the co-ordinate system centered at O_j. The resolution of problem (3) is standard. The coefficients A_{nm}^j and B_{nm}^j are the solutions of the linear system

$$\mathbf{YA} = \tilde{\mathbf{P}}, \tag{4}$$

where $\tilde{\mathbf{P}}$ is the vector (size N) of pressure values on each point M_i, $\mathbf{A}$ is the vector of coefficients to be determined, of size N_a, depending on the truncation order and number of centers O_j, and $\mathbf{Y}$ is the matrix of spherical harmonics of functions associated with each coefficient and computed for each point, its size being $(N \times N_a)$. The least squares solution of this system is unique if $N \geqslant N_a$; its expression is

$$\mathbf{A} = [\mathbf{Y}^*\mathbf{Y}]^{-1}\mathbf{Y}^*\tilde{\mathbf{P}}. \tag{5}$$

For a limited truncation order, $N_j = 2$, say, there are nine terms in the expansion, and as a result $N_a = 9 \times n_c$.

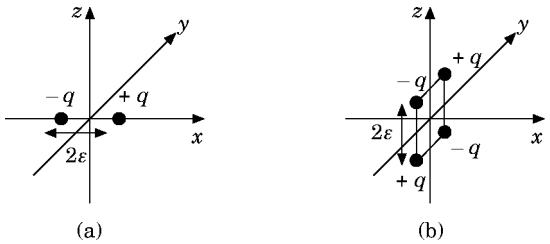

Figure 1. Standard multi-poles: (a) dipole oriented in the (Ox) direction; (b) lateral quadrupole in the (yOz) plane.

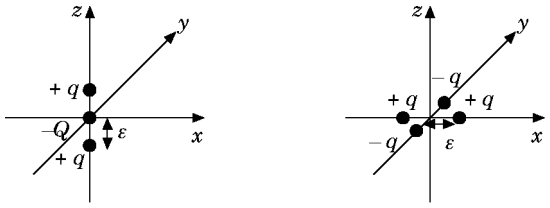

Figure 2. Multi-polar sources associated with the spherical harmonics series terms: (a) $n = 2$, $m = 0$ (A_{20}); (b) $n = 2$, $m = 2$ (A_{22}).

2.2. CORRESPONDENCE BETWEEN THE SERIES TERMS AND MULTI-POLES

It is known [12, 13] that each term in the series (1) or (2) can be identified as the radiation of a multi-polar-type source. However, two terms, A_{20} and A_{22}, do not correspond to a standard multi-polar source (monopole, dipole, longitudinal and lateral quadrupole, some of which are presented in Figure 1). The spatial arrangement and the strengths of these two particular sources are described in Figure 2. The identification of each term of the spherical harmonics series is summarized in Table 1, and the corresponding strength q is given.

In the low frequency range, each multipole can be represented by a set of point sources arranged as in Figures 1 and 2 with ε small with respect to the wavelength. The pressure at each point M from each monopole is

$$p(M) = -\mathrm{i}k\rho cq\, \mathrm{e}^{\mathrm{i}kr}/4\pi r. \tag{6}$$

When all the terms of series (2) are overlaid, several point sources are superposed. For example, the dipole oriented in the (Oz) direction is composed of two monopoles of strength $\pm q$, the multi-pole of Figure 2(a) is composed of three monopoles, the extremes of strength $\pm q$ of which are superposed with the dipole ones. The arrangement shown in Figure 3 was obtained after computing all the strengths, and their sums in certain cases. For a truncation order at $n = 2$ of the spherical harmonics series, 19 monopolar sources are needed to reproduce the primary field. With $n = 1$, the number of sources decreases to seven (numbered 1–7 in Figure 3).

TABLE 1

Examples of equivalent multipoles for $n \leqslant 2$

A_{nm}, B_{nm}	Equivalent multi-poles	Strength q
A_{00}	Monopole	$k_0 A_{00}$
A_{10}	Dipole oriented in (Oz) direction	$k_1 A_{10}$
A_{11}	Dipole (Ox)	$k_1 A_{11}$
B_{11}	Dipole (Oy)	$k_1 B_{11}$
A_{20}	Multi-pole, Figure 2(a)	$q = k_2 A_{20}/2$ $Q = (k_2 - k_0/2)A_{20}$
A_{21}	Lateral quadrupole (xOz)	$k_2 A_{21}/4$
B_{21}	Lateral quadrupole (yOz)	$k_2 B_{21}/4$
A_{22}	Multipole, Figure 2(b)	$k_2 A_{22}$
B_{22}	Lateral quadrupole (xOy)	$k_2 B_{22}/2$

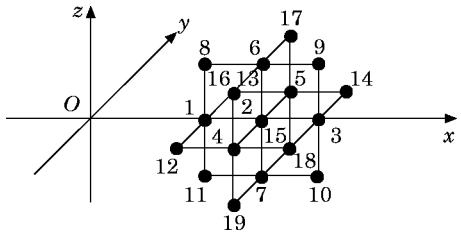

Figure 3. Spatial distribution of the control sources in the general case (nine coefficients A_{nm}, B_{nm}), $n = 2$; one acoustical center in point 2.

2.3. ACTIVE CONTROL APPLICATION

After determination of the complex magnitude of the different monopoles (see Figure 3), the type of active noise control system to choose becomes obvious. One has to replace each monopole by a source of opposite strength. The spatial minimization will depend closely on the accuracy of the primary field representation by series (1) and (2). One thus sees the important role, in the representation's accuracy, of the location chosen for the acoustical center(s) with regard to the geometrical position of the primary source. In references [9, 11], the authors chose acoustical centers near the physical center of the primary sources. Consequently, they obtained good results. For an active control application a further constraint exists: secondary sources cannot be located in the close vicinity of the primary source. Technological constraints (extended primary source, hooding, high temperature, etc.) force one to shift these secondary sources. Thus, the aim of this study was to verify if the spherical harmonics method can be applied for long distances between the primary source and the acoustical center.

In summary, the global approach to determine the best adapted control system for a given primary source is the following: (1) measure at many points of the acoustic field radiated by the primary source in free field; (2) choose one or several acoustical centers where the secondary sources could be placed, taking into account the physical constraints of the problem (use of optimization procedures if necessary [11]); (3) determine the coefficients of the spherical harmonics expansion of the primary field with these acoustical centers; (4) compute the strengths of the real monopoles associated with each coefficient; (5) combine the different monopoles and assign them an opposite phase.

2.4. NUMERICAL SIMULATIONS

2.4.1. *Description of the method*

The method was used to simulate the active control of a primary field for the three following cases of sources: a monopole of unit strength located at the origin O; a dipole oriented in the (Ox) direction of unit moment located at the origin; a complex source composed of five monopoles (an example from reference [14]), the positions and strengths of which are as follows:

Position			Strength
x	y	z	q
0	0	0·201	2 + 2i
−0·201	−0·201	0·101	3 + i
−0·201	0·201	0·01	3 + i
0·2	0·1	0·1	1 + i
0·3	−0·3	−0·2	2 − i

The simulation steps are as follows.

1. The measurement of $\tilde{P}(M_i)$ is simulated by computing the radiation of the primary sources on $N = 210$ points located on the hemisphere of radius three meters and centered at O (see Figure 4). This choice corresponds to the real antenna of microphones which will be used for future experiments (cf., section 4). The spatial distribution of these points is

$$\phi_i = (\pi/15)(i-1),\ i = 1, 2, \ldots, 30, \qquad \theta_i = (\pi/15)(i-1/2),\ i = 1, 2, \ldots, 7.$$

2. Solve the minimization problem (3) for different numbers n_c of acoustical centers, different positions of these centers (cf., Figure 4), and different truncation orders (0, 1 or 2).

3. Compute the strengths of the control sources associated with the spherical harmonics expansion and simulate the secondary field $P_s(M_i)$ at the 210 measurement points.

4. Define a global reduction, GR, by

$$GR = 10 \log \left[\sum_{i=1}^{N} |P_p(M_i)|^2 \Big/ \sum_{i=1}^{N} |P_r(M_i)|^2 \right], \tag{7}$$

where $P_p(M_i)$ is the primary sound pressure at point M_i, $P_s(M_i)$ is the secondary sound pressure, and $P_r(M_i) = P_p(M_i) + P_s(M_i)$ is the residual sound pressure.

2.4.2. *Influence of the distance between primary and secondary sources*

First, it was attempted to assess the influence of the distance d between the primary source at the origin and the center of the secondary sources on the (Ox) axis. For a monopolar primary source, in Figure 5 is shown the reduction, GR, as a function of kd (k is the wavenumber) for a spherical harmonics expansion truncated at orders 0, 1 and 2 to which correspond 1, 7 and 19 secondary sources, respectively. For two acoustical centers located on the (Ox) axis at distance $\pm d$ from the origin, in Figure 6 is shown the global reduction as a function kd for the three types of primary source and a truncation order of 1. Note that, whatever the case, excluding the expansion truncated at order 0,

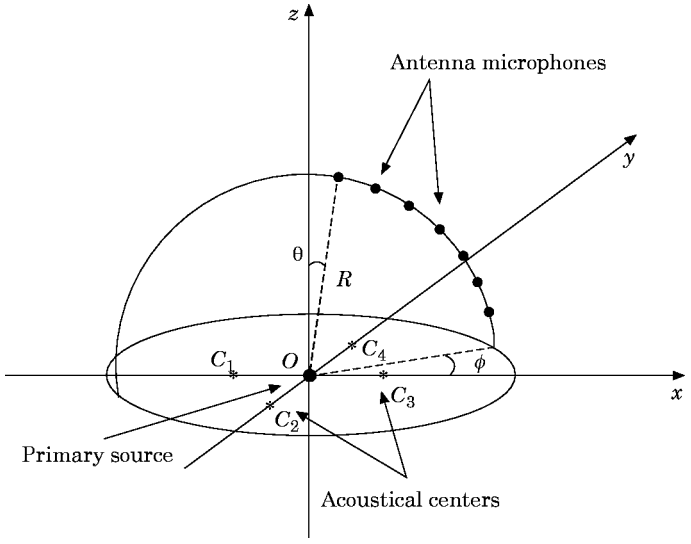

Figure 4. The geometrical arrangement.

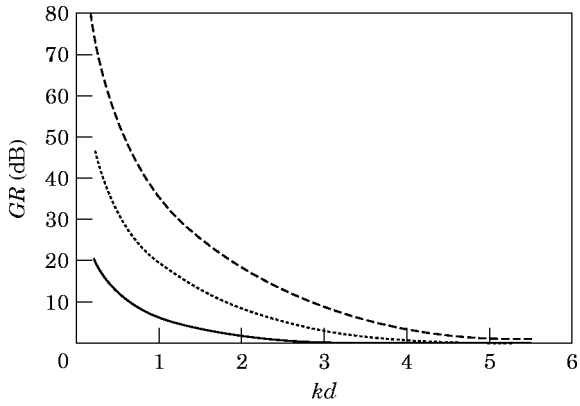

Figure 5. Global reduction as a function of kd: monopolar primary source, one acoustical center. Truncation influence: ——, order 0; ....., order 1; – –, order2.

a global reduction is obtained of more than 10 dB for $kd < 1{\cdot}8$, which corresponds to a 100 Hz frequency and a one m distance d. Further consideration was given to this case exclusively because it corresponds to a realistic practical application of active control of the sound radiated by an electrical transformer. The results obtained for an expansion truncated at order 0 and one acoustical center located at d, and two acoustical centers located at $\pm d$, respectively, are compared in Figure 7 with the theoretical maximum sound power reduction obtained by Nelson [6] for the same configurations. We can see that there is good agreement.

2.4.3. *Influence of the number of secondary sources*

An expansion truncated at order two for one acoustical center gives nine multi-polar terms, and hence 19 monopolar secondary sources. This prohibits practical implementation. Fortunately, the simulation shows that some terms are reduced to zero or are negligible for certain primary sources or acoustical center positions. In Table 2 are shown, for the three types of primary source, the strengths of the different multi-poles obtained for one acoustical center located at 1 m and a 100 Hz frequency. For all the cases, the first seven strengths of the secondary sources predominate. In Table 3 is given the global reduction in decibels with respect to the number of multi-polar sources considered.

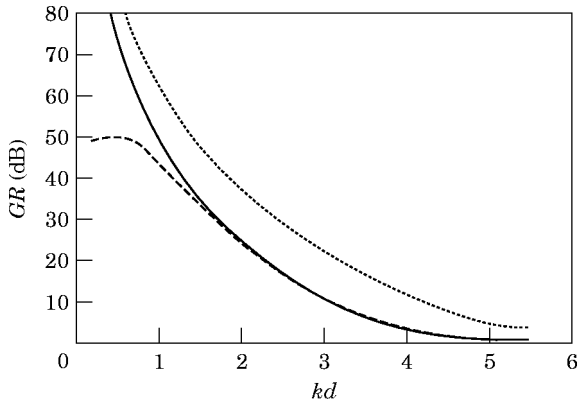

Figure 6. Global reduction as a function of kd: truncated expansion at order 1, two acoustical centers at $\pm d$. Influence on each primary source: ——, monopole; ....., dipole; – –, general source.

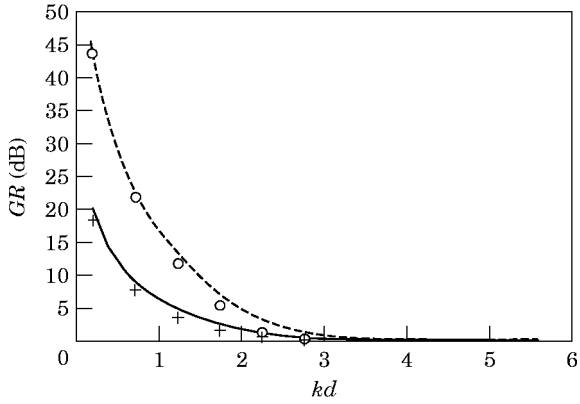

Figure 7. Primary monopole, truncated expansion at order 0: ——, one acoustical center at d; – –, two acoustical centers at $\pm d$. Nelsons results: +, for one secondary monopole $GR = -10 \log (1 - \sin c^2 kd)$ ○, for two secondary monopoles $GR = -10 \log (1 - 2 \sin c^2 kr/(1 + \sin c\, 2kd))$.

TABLE 2

The magnitude at $f = 100$ Hz *of the expansion coefficients* (Pa) *and the corresponding source strengths* ($m^3 s^{-1}$): (a) *primary monopole*, *center at* $x = 1$; (b) *primary dipole*, *center at* $x = 1$; (c) *general primary source*, *center at* $x = 1$

Magnitude	(a)	(b)	(c)
A_{00}	68·13	98·68	860·6
A_{10}	36·52	125	663·8
A_{11}	130·36	62·54	1429·4
B_{11}	0	0	100·5
A_{20}	63·53	124·4	952·5
A_{21}	24·84	62·83	359·8
B_{21}	0	0	16·4
A_{22}	23·47	33·86	293·1
B_{22}	0	0	22·9
Q_1	6·21	6·69	75·08
Q_2	12·9	23·72	191·96
Q_3	3·1	6·8	41·37
Q_4	4·64	6·7	57·53
Q_5	4·64	6·7	58·6
Q_6	5·96	11·28	88·65
Q_7	6·63	13·44	100·33
Q_8	1·23	3·11	17·81
Q_9	1·23	3·11	17·81
Q_{10}	1·23	3·11	17·81
Q_{11}	1·23	3·11	17·81
Q_{12}	0	0	2·27
Q_{13}	0	0	2·27
Q_{14}	0	0	2·27
Q_{15}	0	0	2·27
Q_{16}	0	0	0·81
Q_{17}	0	0	0·81
Q_{18}	0	0	0·81
Q_{19}	0	0	0·81

TABLE 3

The global reduction (dB) *for the three types of primary sources and one acoustical center at* $x = 1$: (a) 19 *sources*; (b) *seven sources*; (c) *three sources*

Primary source	(a)	(b)	(c)
Monopolar	20·5	13	7
Dipolar	10·6	4	−0·5
General	19·2	11·5	5·7

Case (a) corresponds to nine terms and hence to 19 secondary sources, case (b) corresponds to six terms A_{00}, A_{10}, A_{11}, B_{11}, A_{20}, A_{22} and hence to seven secondary sources, and case (c) corresponds to two terms A_{00} and A_{11} and hence to three sources aligned on the (Ox) axis. The suppression of terms degrades the reduction, but in section 3 it is shown how to improve these results by calculating, for a given number of sources, the strengths of these sources by a least squares method, rather than by identification of the coefficients of the truncated spherical harmonics series.

2.4.4. *Influence of the number of acoustical centers*

In Figure 6 it is shown that for two acoustical centers symmetrical with regard to the origin, the reduction obtained is clearly better than for a single center. However, having two centers doubles the number of secondary sources. Nevertheless, it was of interest to verify if, for an approximately equivalent total number of sources, decomposing into many centers provides better results. In Table 4 are shown the following three cases: (a) an expansion truncated at order 2 with one center located 1 m from the primary source on the (Ox) axis, and thus a maximum number of 19 sources; (b) an expansion truncated at order 1 with two centers symmetrical with respect to the origin, at 1 m from the origin, and thus 2×7 sources; (c) an expansion truncated at order 0 with nine centers surrounding the primary source, their spherical co-ordinates being: $(1, \pi/2, 0)$, $(1, \pi/2, \pi/2)$, $(1, \pi/2, \pi)$, $(1, \pi/2, 3\pi/2)$, $(1, \pi/4, \pi/4)$, $(1, \pi/4, 3\pi/4)$, $(1, \pi/4, 5\pi/4)$, $(1, \pi/4, 7\pi/4)$, $(1, 0, 0)$.

Case (c), even though it contained only nine secondary sources, is comparable with cases (a) and (b) because only 11 and 10 sources, respectively, of the 19 and 14 theoretical ones of the two configurations had strengths which have to be taken into account. Case (b) always gave better results than (a) and equivalent to (c). However, the expansion truncated at order 1 with two centers symmetrical in respect to the primary source is more interesting from a practical point of view. In fact, it seems technically preferable to arrange the secondary sources into two groups on each side of the primary source rather than all around it.

TABLE 4

The global reduction (dB) *with respect to the number of centers and the truncation orders*: (a) *order* 2, *one center*; (b) *order* 1, *two centers*; (c) *order* 0, *nine centers*

Primary source	(a)	(b)	(c)
Monopolar	20·5	27·4	29·3
Dipolar	10·6	39·8	20·7
General	19·2	26·8	30·6

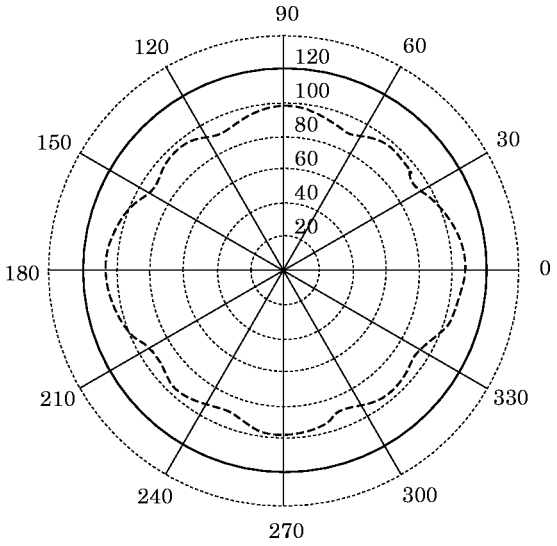

Figure 8. Primary monopole, two acoustical centers at $d = \pm 1$ m, truncated expansion at order 1, $f = 100$ Hz. ——, Sound pressure level before control; – –, sound pressure level after control.

2.4.5. *Spatial distribution of the minimized field*

Here consideration is given to the spatial effect of the minimization in case (b): that is to say, two acoustical centers at a distance of ± 1 m and a truncation order 1 for a primary monopolar source. In Figure 8 are shown the primary and residual (after minimization) sound pressure levels on points belonging to the circle of radius 3 m centered at O and located in the $\theta = \pi/2$ plane. A reduction of more than 20 dB was obtained in all directions. A similar result was observed when the primary and residual sound pressure levels were represented at the 210 points of the antenna (see Figure 9). This result is not specific to the points used for the primary field identification. In Figure 10 it is shown that on the whole plane (xOy), except in the vicinity of the secondary sources, the reduction $A(M)$ computed by equation (8) on a regular mesh ($\Delta x = \Delta y = 0{\cdot}5$ m) was better than 20 dB. In the figure are also indicated preferential directions where the reduction is close to 50 dB:

$$A(M) = 20 \log [|P_p(M)|/|P_r(M)|]. \tag{8}$$

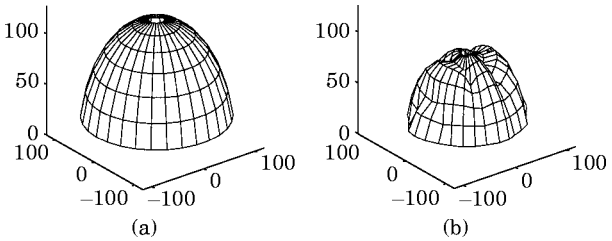

Figure 9. The sound pressure level (a) before and (b) after control on the antenna points (same parameters as Figure 8).

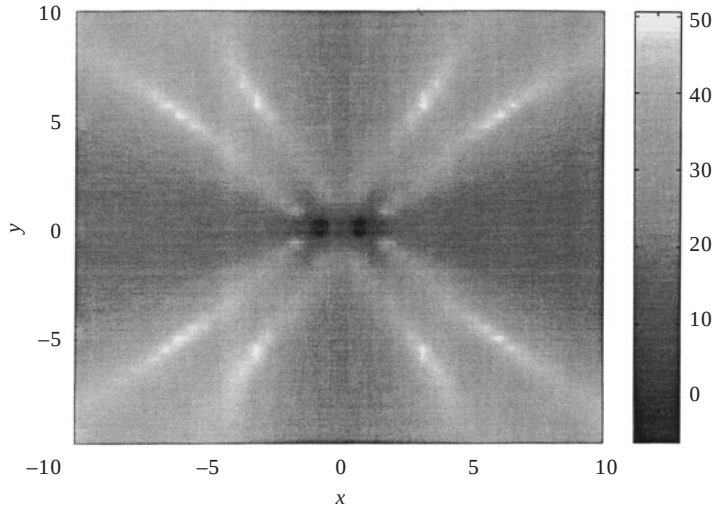

Figure 10. Reduction of the sound level in the $\theta = \pi/2$ plane (same parameters as Figure 8).

3. MINIMIZATION OF THE MEAN SQUARE PRESSURE ON A MICROPHONE NETWORK

The results of the method described in section 2 for the determination of the secondary sources associated with a given primary field provide evidence as to the most advantageous positions of these sources. The method gives a natural arrangement of secondary sources to recompose the primary field and consequently to minimize it. However, the computation of their strengths by this method, called SHM, which is based upon spherical harmonics expansions, has two major disadvantages, as follows.

1. By truncating the series to a given order and retaining only some of the secondary sources, the strength found is no longer optimal for the selected global reduction criterion.
2. Furthermore, one knows that all active control systems in which the strengths of the secondary sources are predetermined and fixed will fail. The system must be adaptive so as to free any given criterion from physical drifts. Moreover, most control algorithms use least squares minimization of the squared pressure at a certain number of error sensors.

In addition, practical realization of multi-poles is not easy and needs fine adjustment. It is easier to drive individual sources than multi-poles. In this section are considered the simulation results obtained by computing the strengths of the secondary sources by a least squares method (called LSM) for the primary sources used in section 2 and the secondary source positions given by the SHM method.

3.1. COMPUTATION PRINCIPLE

Consider N points M_i at which one wants to reduce the acoustic field. Let $P_p(M_i)$ be the primary field at these points. Let S_j be the secondary point sources of strengths q_j $(j = 1, \ldots, S)$.

In active control, the total field at the points M_i is expressed by the vector form

$$\mathbf{P}_t = \mathbf{P}_p + \mathbf{HQ}, \tag{9}$$

where $\mathbf{H}$ is the matrix $(N \times S)$ of elements $h_{ij} = -\mathrm{i}k\rho c\, \mathrm{e}^{\mathrm{i}kd_{ij}}/4\pi d_{ij}$, d_{ij} is the distance between

source S_j and point M_i, $\mathbf{P}_p^{\mathrm{T}} = [P_p(M_1)P_p(M_2)\cdots P_p(M_N)]$, $\mathbf{P}_s = \mathbf{HQ}$ is the secondary field, and $\mathbf{Q}^{\mathrm{T}} = [q_1 q_2 \cdots q_S]$. The quantity to be minimized is

$$J = \sum_{i=1}^{N} |P_t(M_i)|^2. \tag{10}$$

The computation of $\mathbf{Q}$ is standard and leads to the solution

$$\mathbf{Q}_{opt} = -[\mathbf{H}^*\mathbf{H}]^{-1}\mathbf{H}^*\mathbf{P}_p. \tag{11}$$

3.2. SIMULATION RESULTS

3.2.1. *Comparison between the SHM and LSM methods*

Some of the geometrical configurations to which the SHM method had led were considered and the strengths of the associated secondary sources were computed by using formula (11), with N being the 210 antenna points. The results obtained correspond to a reference solution which cannot be implemented but which serves as a reference for comparison with feasible cases. Obviously, the results were highly improved with respect to those obtained by computing the strength by summation of the magnitudes of the different terms of the truncated spherical harmonics series. In Table 5 is shown the reduction obtained by the two methods for the different types of primary sources defined in section 2.4.1. and for different numbers of secondary sources. The modulus of the highest strength for each preceding case is given in Table 6. The two tables lead to the following comments: concentration of a lot of sources into one center gives completely unrealistic strengths; distribution into two centers symmetrical with respect to the primary source significantly improves the results; increasing the number of centers and decreasing the number of sources at each center give very good results and realistic strengths; the discrepancy observed between cases (b) and (c) of Tables 3 and 5 for identical configurations is due to the truncation order, which is 2 and 1, respectively.

TABLE 5

Global reduction (dB): (a) *order* 2, *center at* $x = 1$ (19 *sources*); (b) *order* 1, *center at* $x = 1$ (*seven sources*); (c) *order* 1, *center at* $x = 1$ (*three sources*); (d) *order* 1, *centers at* $x = \pm 1$ (2×7 *sources*); (e) *order* 1, *centers at* $x = \pm 1$ (2×3 *sources aligned on the Ox-axis*)

		Primary source		
		Monopolar	Dipolar	General
(a)	SHM	20·5	10·6	19·2
	LSM	45·5	30·9	43·2
(b)	SHM	9·8	4·1	9·3
	LSM	18·7	9	17·4
(c)	SHM	3·4	−1·5	2·4
	LSM	17·9	8·2	16·3
(d)	SHM	27·4	39·8	26·8
	LSM	57·8	68·3	34
(e)	SHM	23·7	38·5	17·8
	LSM	54·9	67·6	25·2

TABLE 6

The maximum magnitude of the secondary sources ($m^3 s^{-1}$)

		Primary source		
		Monopolar	Dipolar	General
(a)	SHM	12·9	23·7	192
	LSM	2855·3	15 033	43 350
(b)	SHM	1·7	1·7	20·8
	LSM	534·7	1167·9	5251·8
(c)	SHM	1·7	1·4	20·8
	LSM	18·9	30·2	220·5
(d)	SHM	0·8	0·8	9·6
	LSM	27·7	2·5	1010
(e)	SHM	0·8	0·8	9·6
	LSM	3·4	3·4	41·3

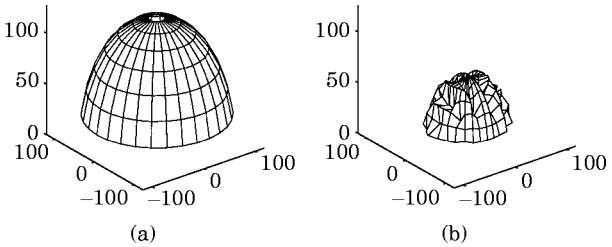

Figure 11. The level (a) before and (b) after control at the antenna points: monopolar primary source, $f = 100$ Hz, two groups of three secondary sources at $d = \pm 1$ m from the primary source.

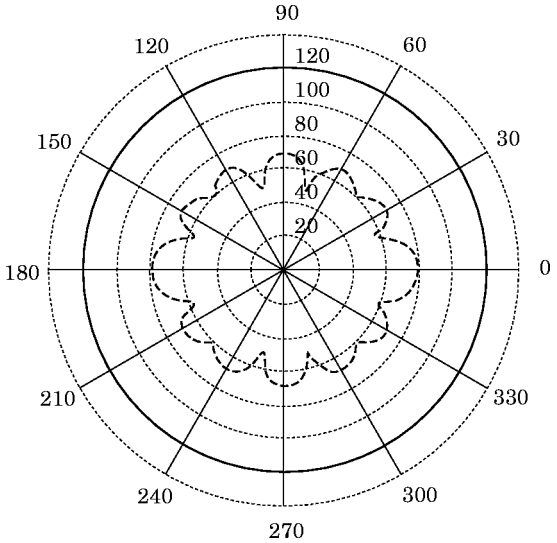

Figure 12. The same source configuration as Figure 11, $f = 100$ Hz: ——, Level before control; – –, level after control.

Configuration (e) is very interesting from a practical point of view: it includes only six secondary sources, the minimum reduction is 25 dB (for the complex primary source) and the source strengths are realistic.

3.2.2. *Spatial distribution*

The same type of graphical representation as in section 2.4.5. is given for configuration (e) and a monopolar primary source (see Figures 11–13).

As shown in Figure 13(a), a reduction of more than 40 dB was obtained on the whole plane, with preferential directions where 80 dB is reached. Using these directions to optimize the placement of a restricted number of error sensors will be described in the following section. The influence of the frequency and the distance between primary and secondary sources are shown in Figure 13(b). Note that the reduction was always better than 20 dB for $kd < 3$.

3.3. REDUCTION OF THE NUMBER OF ERROR SENSORS

After one finds a compromise between the number of sources and the reduction obtained, the next step is to decrease the number of error sensors. It is not always possible to measure totally the acoustic field all around the primary source. Furthermore, for the implementation of a real time control algorithm, the number of error sensors must be limited, but it must remain greater than the number of secondary sources. It is thus

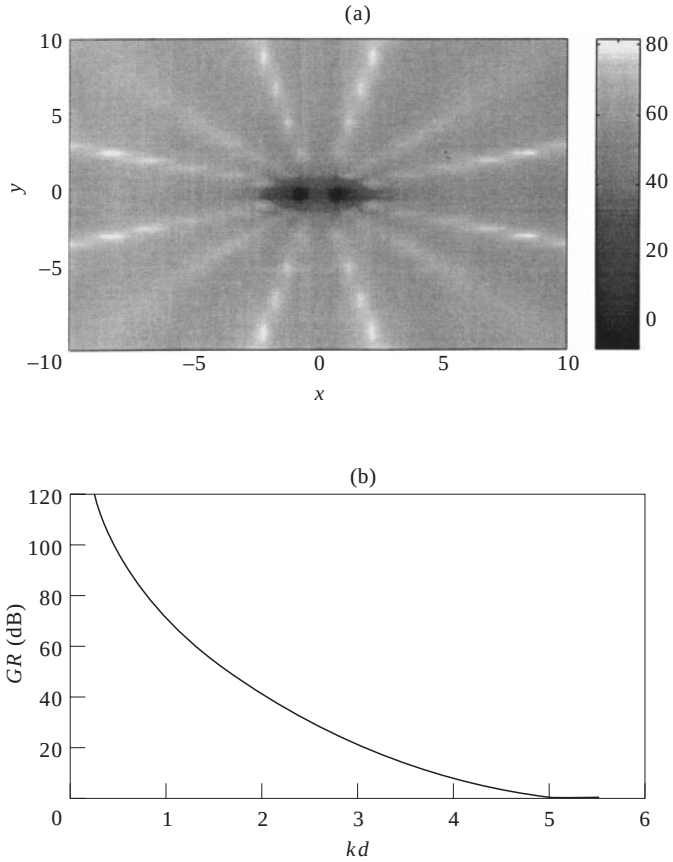

Figure 13. (a) Reduction in the $\theta = \pi/2$ plane. (b) Global reduction.

important to establish what the preceding results become when the number of error sensors is decreased from 210 to a few units. The difficulty is in choosing the positions of these sensors. It is clear that these positions are directly linked with the objective sought. If the aim is to execute a directional control, then the sensors are concentrated in the chosen directions. On the other hand, if the initial objective is to provide a three-dimensional control, the choice of the sensor positions become primary and delicate.

3.3.1. *Proposed procedure*

The optimization of the sensor positions can be treated in different ways. One can use gradient methods or systematize a computation taking into account the different combinations of N sensors among the first 210. However, such strategies are difficult to implement in a three-dimensional problem. Computation times are long and the problems are often non-convex. Without excluding these methods, in the first instance one can opt for a simpler method based on an observation. During the simulations, it was observed that, for the monopolar and dipolar primary sources, the minimization with N secondary sources makes preferential directions for which the reduction is maximum appear in the (xOy) plane (see Figure 13(a)). We have not yet completely studied this phenomenon, but it nevertheless seems of interest to locate the error sensors in these directions. Snyder and Hansen [15] observed the same thing for a vibrating panel radiation problem.

In summary, the following procedure is proposed: (1) solution of the minimization problem (10) for $N = 210$ and S secondary sources (called optimal control); (2) computation and graphical representation of the residual sound pressure level (after optimal control) on the circle of radius 3 m in the $\theta = \pi/2$ plane; (3) marking of the co-ordinates of the $N \geqslant S$ points of minimum residual level; (4) solution of equation (10) for the N positions of sensors defined in step (3); (5) estimation of the efficiency of the chosen configurations; (6) comparison of the secondary source strengths in the reference case ($N = 210$) and the feasible case ($N \geqslant S$).

3.3.2. *Results*

In Figure 14 is shown the residual level in the $\theta = \pi/2$ plane, 3 m away from the origin

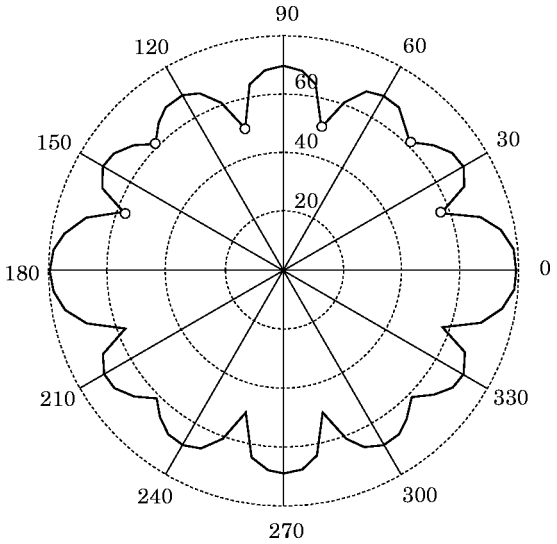

Figure 14. The level after optimal control (210 sensors), primary monopole, same configuration as Figure 11.

TABLE 7

Global reduction (dB) *and secondary source magnitude* ($m^3\ s^{-1}$)

	210 sensors, $GR = 54{\cdot}9$ dB	six sensors, $GR = 53{\cdot}7$ dB
Q_1	2·76	2·75
Q_2	3·41	3·38
Q_3	1·14	1·13
Q_4	2·76	2·75
Q_5	3·41	3·38
Q_6	1·14	1·13

for the configuration (e) and a monopolar primary source. The symbols "○" mark the points of minimum residual level. The minimization problem (10) was solved on the basis of these points. In Table 7 the results obtained are compared with those of the reference case with 210 points.

The global reduction and the secondary source strengths differed only slightly for $N = 210$ and $N = 6$ sensors. Conversely, when the sensors were positioned on the basis of the directions of minimum reduction, noise reduction was weaker. One now needs to systematize the procedure and, in particular, find a rule to localize the directions of maximum reduction in the general case. This would then constitute a simple method of error sensor location.

4. CONCLUSION AND PERSPECTIVES

A procedure has been proposed which may improve the implementation of an active control system of the noise radiated by sound sources in free field. Decomposing this sound field on a spherical harmonics basis with one or several centers shifted from the geometrical center of the source allows one to estimate the number and realistic arrangement of secondary sources likely to minimize the primary field. After locating the secondary sources, one uses a least squares method to compute their strengths. The simulations showed a global reduction in the whole space at low frequencies even when long distances separated the real acoustical center of the primary source and those of the secondary sources. An interesting configuration of secondary sources has been made apparent, constituted of 2×3 sources arranged symmetrically with respect to the primary source and aligned along an axis passing through this source. Associated with six suitably placed error sensors, the configuration gave very good results for the simulated monopolar and dipolar primary sources. The theory of the geometrical arrangement of the directions of maximum reduction should be further investigated.

An experimental implementation of the proposed method will soon be undertaken for a mean voltage transformer. For this practical application a certain number of elements still need to be studied: the influence of a reflecting ground; the influence of the diffraction of secondary source radiation by an extended primary source; wind-provoked degradation in the far field; degradation of the results when the primary source radiates in an enclosed space rather than in free field.

REFERENCES

1. W. B. CONOVER and R. J. RINGLEE 1955 *Transactions of the AIEE part III, Power Apparatus and Systems* **74**, 77–90. Recent contributions to transformer audible noise control.

2. K. KIDO and S. ONODA 1972 *Science Reports of the Research Institutes*, *Tohoku University* (*RITU*), *Technical Report* **23**. Automatic control of acoustic noise emitted from power transformer by synthesizing directivity.
3. C. F. ROSS 1978 *Journal of Sound and Vibration* **61**, 473–480. Experiments on the active control of transformer noise.
4. N. HESSELMANN 1978 *Applied Acoustics* **11**, 27–34. Investigation of noise reduction on a 100 kVA transformer tank by means of active methods.
5. M. J. M. JESSEL and O. L. ANGEVINE 1980 *Proceedings Internoise* '80, 689–694. Active acoustic attenuation of a complex noise source.
6. P. A. NELSON, A. R. D. CURTIS, S. J. ELLIOTT and A. J. BULLMORE 1987 *Journal of Sound and Vibration* **116**, 397–414. The minimum power output of free field point sources and the active control of sound.
7. P. A. NELSON and S. J. ELLIOTT 1992 *Active Control of Sound*. London: Academic Press.
8. A. J. KEMPTON 1976 *Journal of Sound and Vibration* **48**, 475–483. The ambiguity of acoustic sources—a possibility for active control?
9. P. J. T. FILIPPI, D. HABAULT and J. PIRAUX 1988 *Journal of Sound and Vibration* **124**, 285–296. Noise sources modeling and intensimetry using antenna measurement and identification procedures.
10. P. J. T. FILIPPI, and J. PIRAUX 1985 *Journal of Sound and Vibration* **98**, 596–600. Noise sources modeling and identification.
11. J. PIRAUX 1987 *Thèse d'État*, *Université d'Aix-Marseille II*. Application des méthodes actives au contrôle d'un champ acoustique.
12. P. M. MORSE and H. FESHBACH 1953 *Methods of Theoretical Physics* (volumes 1 and 2). New York: McGraw-Hill.
13. P. M. MORSE and K. U. INGARD 1968 *Theoretical Acoustics*. New York: McGraw-Hill.
14. F. LAVILLE, M. SIDKI and J. NICOLAS 1992 *Acustica* **76**, 193–198. Spherical acoustical holography using sound intensity measurements: theory and simulation.
15. S. D. SNYDER and C. H. HANSEN 1991 *Journal of Sound and Vibration* **148**, 537–542. Using multiple regression to optimize active noise control system design.